Science in China Ser. D Earth Sciences 2005 Vol.48 Supp. I 74—84

Comparison of flux measurement by open-path and close-path eddy covariance systems

SONG Xia[1,2], YU Guirui[1], LIU Yunfen[1], SUN Xiaomin[1], REN Chuanyou[1,2] & WEN Xuefa[1,2]

1. Chinese Ecosystem Research Network Synthesis Research Center, Institute of Geographic Sciences and Natural Resources Research, Chinese Academy Sciences, Beijing 100101, China;
2. Graduate School of the Chinese Academy of Sciences, Beijing 10039, China

Correspondence should be addressed to Yu Guirui (email: yugr@igsnrr.ac.cn)

Received July 14, 2004; revised January 13, 2005

Abstract For flux measurement, the eddy covariance technique supplies a possibility to directly measure the exchange between vegetation and atmosphere; and there are two kinds of eddy covariance systems, open-path and close-path systems. For the system error, it may result in difference of flux measurements by two systems. Therefore, it is necessary to compare the measured results from them. ChinaFLUX covers of eight sites applied the micrometeorological method, in which Changbai Mountains (CBS) and Qianyanzhou (QYZ) carried out open-path eddy covariance (OPEC) and close-path eddy covariance (CPEC) measurements synchronously. In this paper the data sets of CBS and QYZ were employed. The delay time of close-path analyzer to the open-path analyzer was calculated; the spectra and cospectra of time-series data of OPEC and CPEC were analyzed; the open-path flux measurement was used as a standard comparison, the close-path flux measurement results were evaluated. The results show that, at two sites the delay time of CO_2 density for close-path analyzer was about 7.0—8.0 s, H_2O density about 8.0—9.0 s; the spectrum from the open-path, close-path and 3D sonic anemometer was consistent with the expected –2/3 slope (log-log plot), and the cospectra showed the expected slope of –4/3 in the internal subrange; the CO_2 flux measured by the close-path sensor was about 84% of that of open-path measurement at QYZ, about 80% at CBS, and the latent heat flux was balanced for two systems at QYZ, 86% at CBS. From the flux difference between open-path and close-path analyzers, it could be inferred that the attenuation of turbulent fluctuations in flow through tube of CPEC affected H_2O flux more significantly than CO_2 flux. The gap between two systems was bigger at CBS than at QYZ; the diurnal variation in CO_2 flux of two measurement systems was very consistent.

Keywords: eddy covariance technique, open-path eddy covariance, close-path eddy covariance, delay time, spectrum analyze, flux.

DOI: 10.1360/05zd0007

The first application of the eddy covariance method measuring carbon dioxide exchange occurred in the early 1970s[1,2]. Initial studies were performed over corn using a propeller anemometer and a modified, close-path analyzer, with a capacitance detector. The time constants of these sensors, however, were

relatively slow (2 Hz). These limitations prompted for the availability of sonic anemometers and the development of rapid-responding[3–6], open-path and close-path infrared gas analyzers were able to sense CO_2 fluctuations as rapidly as ten times per second. Gradually, the eddy covariance technique (including open-path analyzer and sonic anemometer or close-path analyzer and sonic anemometer) became a prevalent mean for measuring net carbon dioxide exchange. The two different eddy covariance systems (OPEC and CPEC) were perfected little by little, however, they still have limitations too, including applicable over special environment, routine maintenance, and the different observing results of two systems. As we know, the fasting-response is the main privilege of OPEC, however, they can't be exposed to rain because of their imperfect waterproofing, and need extensive maintenance for constant operation. For long-term measurement, open-path analyzers are often unreliable. On the other hand, using close-path analyzers, the stability and accuracy of measurement, the simplicity of operation, and the convenience of periodic calibration using standard gas, with these advantages, a close-path analyzer is suitable for long-term measurements, however, to make a continuous measurement of the atmospheric CO_2 with a close-path analyzer, we have to draw the sample air using an air pump into a sample cell in the analyzer through a sampling tube. This sampling process causes attenuation of fluctuations in CO_2 concentration, which then lead to the underestimation of CO_2 flux. Currently, the open-path eddy covariance and close-path eddy covariance are parallel means in FLUXNET measurement, but the dominating application occurred, such as CPEC in AsiaFlux, CPEC and OPEC in Ameri-Flux, CPEC in Euro-Flux, OPEC in Ko-Flux.

The system error between OPEC and CPEC may result in different flux outcomes, therefore, it is necessary to compare the measurement results of two systems[7–12]. The early study with OPEC and CPEC two systems had a problem[8–12], the instruments of two system came from different companies, which easily resulted in significant system error. ChinaFLUX installed OPEC and CPEC synchronously at sites CBS and QYZ, and the instruments of two systems were produced in the same Manufacturer and the model was completely the same. The observation by two different systems can supply a feasible means for forest flux measurement, at the same time, for the synchronous of two systems, they can compensate the missing data each other. The main objectives of this paper are: (1) to confirm the delay time of close-path analyzer, (2) to qualify the data of OPEC and CPEC and to evaluate the reliability of measurement results by spectral analyses, and (3) to compare CO_2 flux of OPEC and CPEC, then to analyze the difference of two eddy covariance systems.

1 Theory

1.1 Eddy covariance measurement

The eddy covariance technique becomes a standard means of measuring net carbon dioxide exchange[13]. The equation defining the conservation of mass provides the theoretical guide for utilizing the eddy covariance technique[14,15]. As shown in fig. 1 the conservation of mass states that the time rate of change of the CO_2 mixing ration, c , is balanced by the sum of the flux divergence of CO_2 in the vertical (z), lateral (x) and longitudinal (y) directions and the biological source sink-strength (S_B), and the expression is

$$\frac{dc}{dt} = -\left(\frac{\partial Fz}{\partial z} + \frac{\partial Fx}{\partial x} + \frac{\partial Fy}{\partial y} + S_B(x, y, z)\right). \quad (1)$$

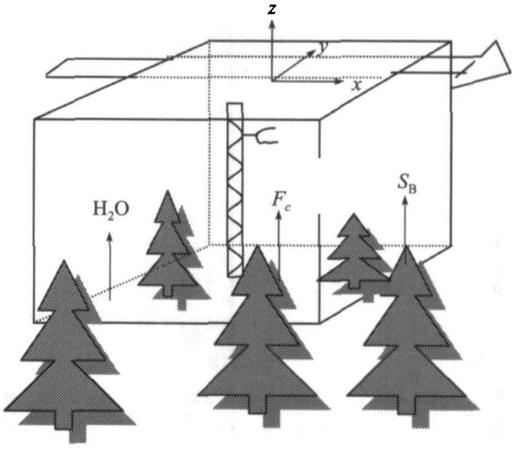

Fig. 1. CO_2 exchange in a unit volume between vegetation and atmosphere.

The mixing ration of CO_2, c, is defined as the ratio of mole density of CO_2 to the mole density of dry air, F denotes the flux density of CO_2 (μmol m^{-2} s^{-1}). There are several assumptions when eddy covariance was applied in practice, the atmosphere steady, underlying surface horizontally homogeneous and on flat terrain. Based on these assumptions, the conservation equation simplifies to a balance between the vertical flux divergence of CO_2 and its biological source/sink strength, S_B:

$$\frac{\partial Fz}{\partial z} = -S_B(z). \tag{2}$$

By integrating eq. (2) with respect to height, one derives an equality between the mean vertical flux density measured at some height, $F_c(h)$, and the net flux density of material in and out of the underlying soil, $F_c(0)$, and vegetation:

$$F_c(h) = F_c(0) - \int_0^h S_B(Z)\mathrm{d}z. \tag{3}$$

On the basis of physical principles and Reynolds' rules of averaging[16], the mean covariance between vertical velocity (w) and the CO_2 mixing ration, c, produces a direct measurement of the mean vertical flux density of CO_2:

$$F_c = \overline{\rho_a wc} \cong \overline{\rho_a w'c'}: \tag{4}$$

In eq. (4), the overbars denote time averaging and primes represent fluctuations from the mean. A positively signed covariance represents net CO_2 transfer into the atmosphere and a negative value denotes the reverse.

1.2 Water and heat adjustment

In practice, CO_2 is measured with infrared spectrometers, which do not measure mixing ration, c. Instead they sample molar density, ρ_c (moles per unit volume). In principle, changes in molar density can occur by adding or removing molecules in a controlled volume or by changing the volume, as is done when pressure, temperature and humidity change in the atmosphere. By measuring the eddy flux covariance in terms of molar density, the net flux density of CO_2 across the atmosphere-biosphere interface is evaluated as

$$F_c = \overline{w\rho_c} = \overline{w'\rho_c'} + \overline{w}\,\overline{\rho_c}. \tag{5}$$

The new term, on the right hand side of eq. (5) is the product of the mean vertical velocity and CO_2 density. The mean vertical velocity arises from density fluctuation, its magnitude is too small (<1 mm/s) to be detected by anemometry, but it can be computed using the Webb-Pearman-Leuning :

$$F_c = \overline{w'\rho_c'} + \frac{m_a}{m_v}\frac{\overline{\rho_c}}{\overline{\rho_a}}\overline{w'\rho_v'} + \left(1 + \frac{\overline{\rho_v} m_a}{\overline{\rho_a} m_v}\right)\frac{\overline{\rho_c}}{\overline{T}}\overline{w'T'}, \tag{6}$$

where m_a is the molecular weights of air, and m_v water vapor. Eq. (6) ignores effects of pressure fluctuations, which may be significant under high winds[18] and advection[20]. Significant terms in eq. (6) depend on whether one uses an open or closed path infrared spectrometer. If one draws air down a heated tube in a turbulent state, as is needed to implement a close-path sensor, temperature fluctuations will dampen and approach zero, thereby canceling the last term on the right hand side of eq. (6)[14−19].

1.3 Spectrum analysis

As to the spectral analysis, it studies the period oscillation by the time serial. We can consider the time serial as a complex oscillation track, and we can study the serial internal structure, thereby, knowing how the energy was contained at individual frequency.

Suppose a stable time serial in (0, T), and the Fourier transforms is

$$X(t) = \sum_{k=0}^{\infty}[a_k \cos\omega_k t + b_k \sin\omega_k t]. \tag{7}$$

Equation (7) is a spectral expanding of randomly process $X(t)$, and it showed that, a stable process can be analyzed by numerous co-oscillation at different frequency. Eq. 7 is just a discrete stable processing of $X(t)$, and it will become a continuous spectrum when $T \to \infty$. In practice, the spectrum includes power spectrum and cospectrum. The so-called power spectrum is spectrum density, since it is the mean power

distribution of a single time serial in frequency f, and it shows how the co-swing contributes to the total swing. For two time serials the co-spectrum is how the component distributing at individual frequency contributes to their covariance, thereby, we can discern whether there are some relationships between two time serials, and then we can know which oscillation component is the most important control to their covariance.

2 Sites and observing system

2.1 Sites

The experimental sites are located in the QYZ and CBS experimental station, CAS. The ecological experimental station QYZ (115°04′13″E, 26°44′48″N) is situated on the typical red earth hilly region in the mid-subtropical monsoon landscape zone of South China. According to the statistics of meteorological data from 1985—2002, the mean annual temperature is 17.9℃, annual precipitation 1542.4 mm, annual evaporation 1110.3 mm, mean relative humidity 84%. The coniferous forest plantation was mainly planted after 1985. The forest canopy is dominated by *Pinus massoniana Lamb*, *Pinus elliottii Engelm*, *Cunninghamia lanceolata Hook*, *Schima crenata Korthals*, *Citrus* L., etc. The area of evergreen vegetation is about 76% of the total area. The experimental site of CBS is performed in the number one sample plot (42°24′N, 128°6′E). The slope of terrain is not larger than 4%. The Changbai Mountains belongs to the temperature continental climate, mean annual temperature –7.3—4.9℃, mean annual precipitation 600—900 mm. The forest canopy are dominated by *Pinuskoriaensis*, *Tiliaamurensis*, *Quercusmongolica*, *Fraximusmandshurica*, *Acermono.*, etc. The coverage of underlayer shrub is 40%, dominated by *corylusmandshurica*, *Lonicerachrysantha*, *Philadelphusschrenkii*, *Deutziaamurensis*, and the coverage of grass is 70%, dominated by *Brachybotrysparidoformis*, *Carexsideroticta*, *Equisetumhiemale.*, etc.[22—24].

2.2 Observing system

On the measurement tower, the eddy covariance system includes routine meteorology system, seven-level profile CO_2 and H_2O system, OPEC, and CPEC in two sites. The analyzers of OPEC and CPEC are described in table 1. Fig. 2 shows the schematic of close-path and open-path systems. In two sites, the OPEC and CPEC were installed at the same height, 23 m in QYZ, and 41.4 m in CBS. The sample tube of CPEC is 29.3 m long, in QYZ, and 55.5 m in CBS, with the same 0.5 mm inner diameter. And the type and model of instruments are the same in two sites.

The eddy covariance system (OPEC and CPEC) consists of the following components: 3-D sonic anemometer (Campbell Scientific, Inc.), CSAT3, close path infrared gas analyzer (LI-COR, Inc.), LI7000, open path infrared gas analyzer (LI-COR, Inc.), LI7500, data logger (Campbell Scientific, Inc.), CR5000, temperature and humidity sensor (Vaisala), HMP45C. The datalogger program controls the system, measures all input variables and calculates on-line fluxes that are stored on a PCMCI card and can be displayed real time on the dataloger's LCD or on a PC screen. Raw time series data at 10 Hz are also stored for diagnostic and post-processing purposes.

Table 1 Specifications comparison of CPEC and OPEC analyzers

Specifications	LI7500 (OPEC)	LI7000 (CPEC)
Type	Absolute, non-dispersive infrared gas analyzer	Differential, non-dispersive infrared gas analyzer
Temperature range/℃	–25—50	0—50
Power requirements/V	10.5—30 DC	100—240 AC
CO_2 range (10^{-6})	0—3000	0—3000
CO_2 zero drift with temperature/-10^{-6}℃$^{-1}$	± 0.1	± 0.3
CO_2 span drift/r℃$^{-1}$	± 0.02%	± 0.2%
H_2O range/mmolmol^{-1}	0—60	0—60
H_2O zero drift with temperature/mmol mol^{-1}℃$^{-1}$	± 0.03	± 0.02
H_2O span drift/r℃$^{-1}$	± 0.15%	± 0.4%

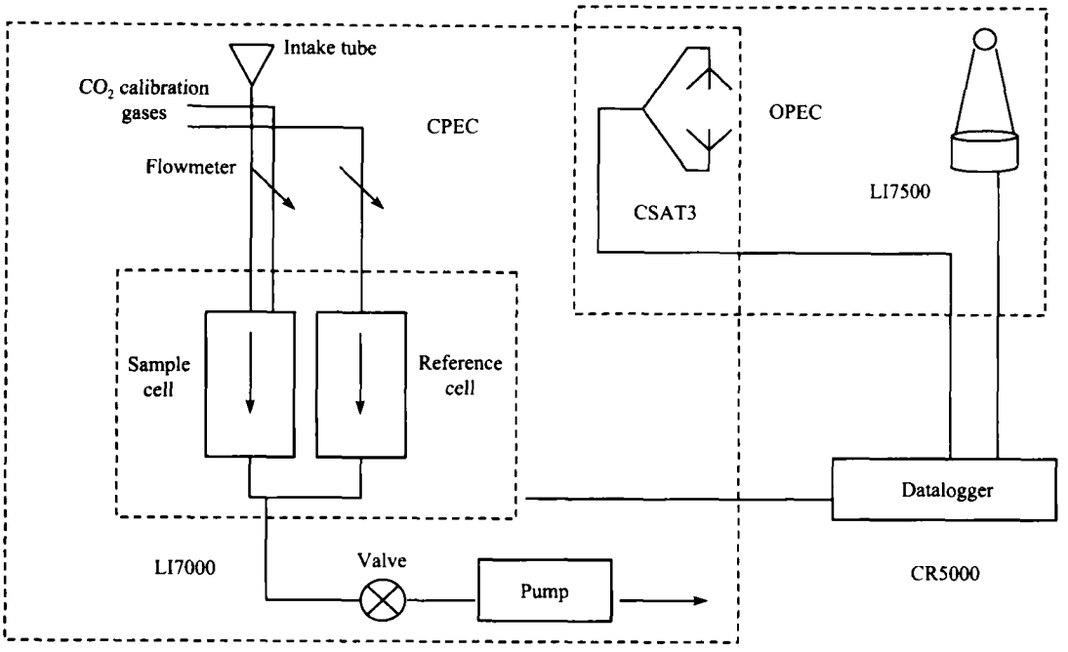

Fig. 2. Schematic of the close-path and open-path CO_2 system.

The system uses a high capacity diaphragm vacuum pump, and it can achieve an open volume flow rate of 5 m^3/h at standard conditions. There are four filters in this system: one filter at the sample intake, 47 mm diameter, 10 μm pore size and mounted in an aluminum filter holder; one filter just upstream from the sample cell of the analyzer 47 mm diameter and 2 μm pore size, mounted in an aluminum holder also; one Gelman filter cartridge assembly 50 mm, 1 μm pore size upstream of the reference cell; and one filter for the air that enters the scrub chemicals, 25 mm diameter, 1 μm pore size, mounted in a Delrin open end filter holder.

The calibration system is to compensate for any offset drifts and changes in the gain in the concentration measurements due to temperature, contamination in the optical path, light source and detector aging. It allows three gases with known concentration to flow into the sample cell of the analyzer to perform automatic calibration at user defined intervals. For convenience, two polycarbonate bottles, one filled with Decarbide (CO_2 scrubber) and the other with magnesium perchlorate (H_2O scrubber) can provide zero gas for the routine operation and during offsets and gain adjustments. The bottles with the chemicals are connected in a closed loop with the reference cell. The internal pump of the LI7000 circulates air continuously between the chemicals and the reference cell so that all the CO_2 and water vapor are removed form the stream.

3 Results and discussions

3.1 Delay time for CO_2 and H_2O

Because of the finite length of the intake line, there is a certain time lag between the wind measurements made by the anemometer and the concentration measurements made by the IRGA, and this lag time is so-called delay. One of the requirements of the eddy covariance method is that all measurements have to be made synchronously, in order to decrease the system error, OPEC and CPEC, the two observing systems, only use one 3-D sonic anemometer. To determine the lag time precisely is the basis to obtain the exact flux.

The lag time was determined by finding the

maximum covariance between the vertical wind and CO_2 (H_2O) concentration (by shifting the two time series)[7,8,10,11]. A good reliable estimation of the tube delay could be obtained during periods of the day when the CO_2 and H_2O fluxes are strong and the peaks are sharp and well defined. We used the time series data between 14:00—15:00 to calculate delay time. In QYZ the delay for CO_2 and H_2O was about 7.0 s and 8.5 s respectively, and it was 7.9 s and 8.3 in CBS (fig. 3). In the two sites, for the increased interaction of water vapor with the internal surfaces of the tubing, the delay of H_2O was larger than CO_2. Because the instruments are on the same type and model, the delay time of the same gas is determined by the length of the intake tube, consequently, the delay of CO_2 in QYZ was smaller than that in CBS, however, the delay of H_2O in QYZ was larger than that in CBS; it was probably caused by the high H_2O concentration in QYZ. And the phenomenon needs to be further studied.

The delay time depends primarily on the actual flow rate of air, the length of the intake line, the inside diameter of the tube and the internal volumes of the components in the sample intake line like filters, connectors, etc. For the same instruments, the delay time was similar in the two sites.

3.2 Spectral analysis

In order to test the frequency response of eddy covariance system sensors, as well as to gain information on the physical structure of eddies, we analyzed the power spectrum and cospectrum of measurement term. A time serial was considered as a complex oscillation track, and then it could be always analyzed by numerous co-oscillation at individual frequency, thereby knowing how the frequency contributes to the oscillation by observing the frequency distribution, and it is so-called spectral analysis[26]. In this study, the power spectral density, $S_s(f)$, of the time series of s, and the co-spectral or cross-spectral density of s and w, $C_{ws}(f)$, were estimated using Welch's averaged periodogram method. For both spectral densities, a fast Fourier transform length of 2^9 was used with nonoverlapping Hanning windows of the same length. One hour of the high-frequency data were used, thus, all time series consisted of 36000 values, detrended by removing the mean. Both spectral densities were multiplied by f to enhance the higher frequencies, and $S_s(f)$ and $C_{ws}(f)$ were standardized by the variance of s and the absolute value of the covariance between w and s, respectively.

The power spectra of ρ_{CO_2}, w, u, v were analyzed (fig. 4). The spectrum of ρ_{CO_2} showed that, the two

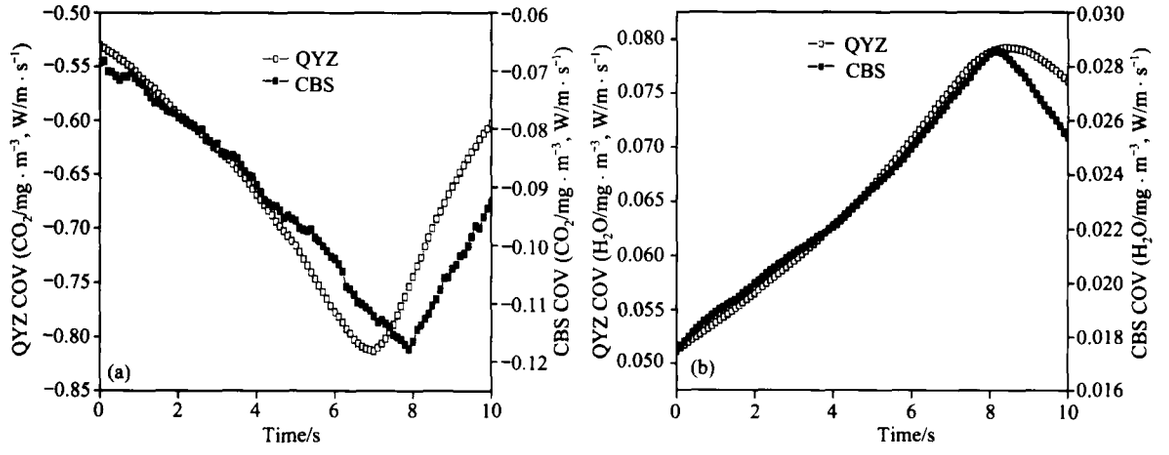

Fig. 3. The delay for CO_2 and H_2O determined by the maximum covariance between the vertical wind and CO_2 (H_2O) concentration. (a) The lag time for CO_2; (b) the lag time for H_2O.

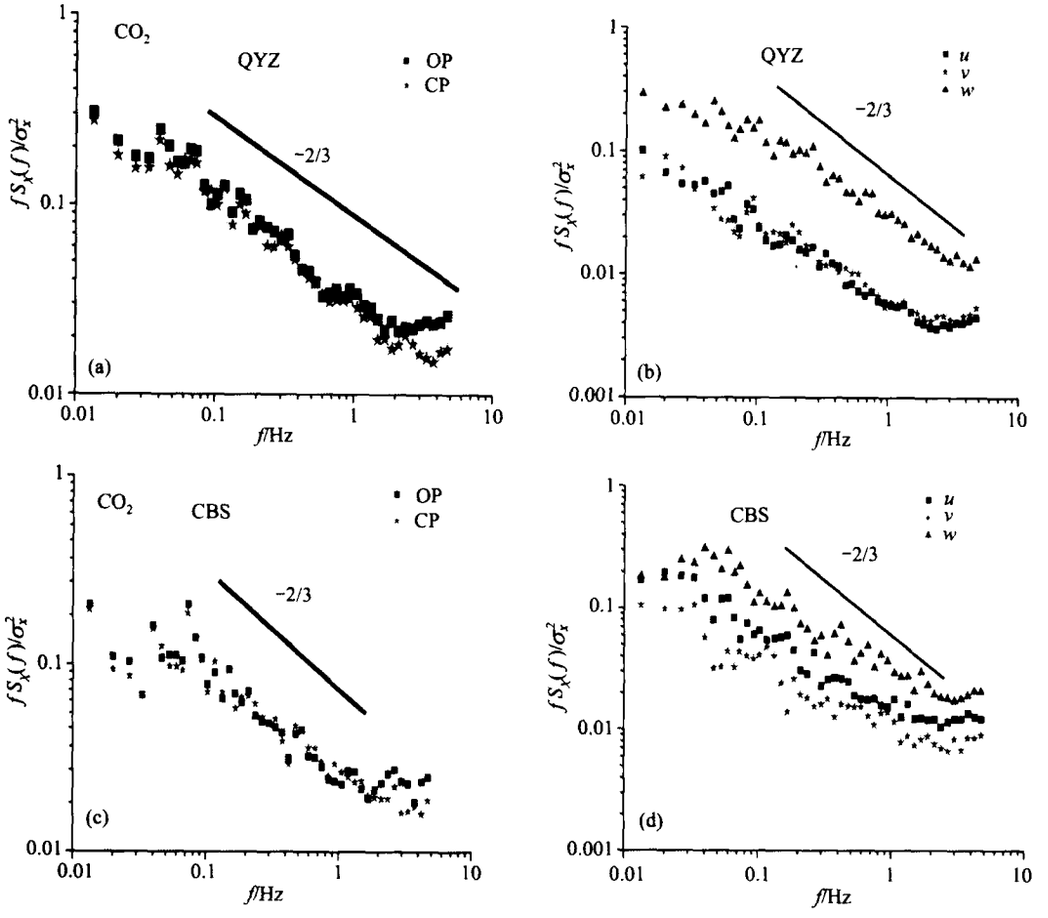

Fig. 4. The power spectrum of ρ_{CO_2}, w, u, v of OPEC and CPEC (X in (a) and (c) is CO_2 density, u, v, w in (b) and (d) is 3-D wind speed).

analyzers of OPEC and CPEC were similar at all frequencies, however, the spectrum of CPEC was a slight drop. The power spectrum of ρ_{CO_2}, w, u, v exhibited the expected –2/3 slope, which has been used to examine the structure of turbulence over oceans[26]. Because the sampling tube that was used to supply air to the close-path analyzer acts as a high frequency filter, spectrum power in the CO_2 signal from the close-path analyzer was lost at $f > 2$ Hz, however Leuning and Yasuda showed that there was a rapid decrease in spectral density for the close-path analyzer for $f > 0.1$ Hz.

The two cospectra, vertical wind speed and CO_2 density, vertical wind speed and sonic anemometer temperature, are shown in fig. 5 (log-log plot). All the cospectra showed the expected slope of –4/3 in the inertial subrange. The cospectrum of vertical wind speed and CO_2 density was consistent with the cospectrum vertical wind speed and sonic anemometer temperature at all frequencies. If we assume that the fine-wire thermometer approximates an ideal sensor with respect to frequency response, fig. 5(a), (c) show that there was no significant loss in the measured CO_2 flux due to separation between the open-path analyzer and the sonic anemometer.

The comparison of cospectrum or vertical wind speed and CO_2 density of CPEC and OPEC is shown in fig. 5 (log-log plot). The cospectra showed the expected slope of –4/3 in the inertial subrange. When $f > 1$ Hz, signals of CPEC were very consistent with

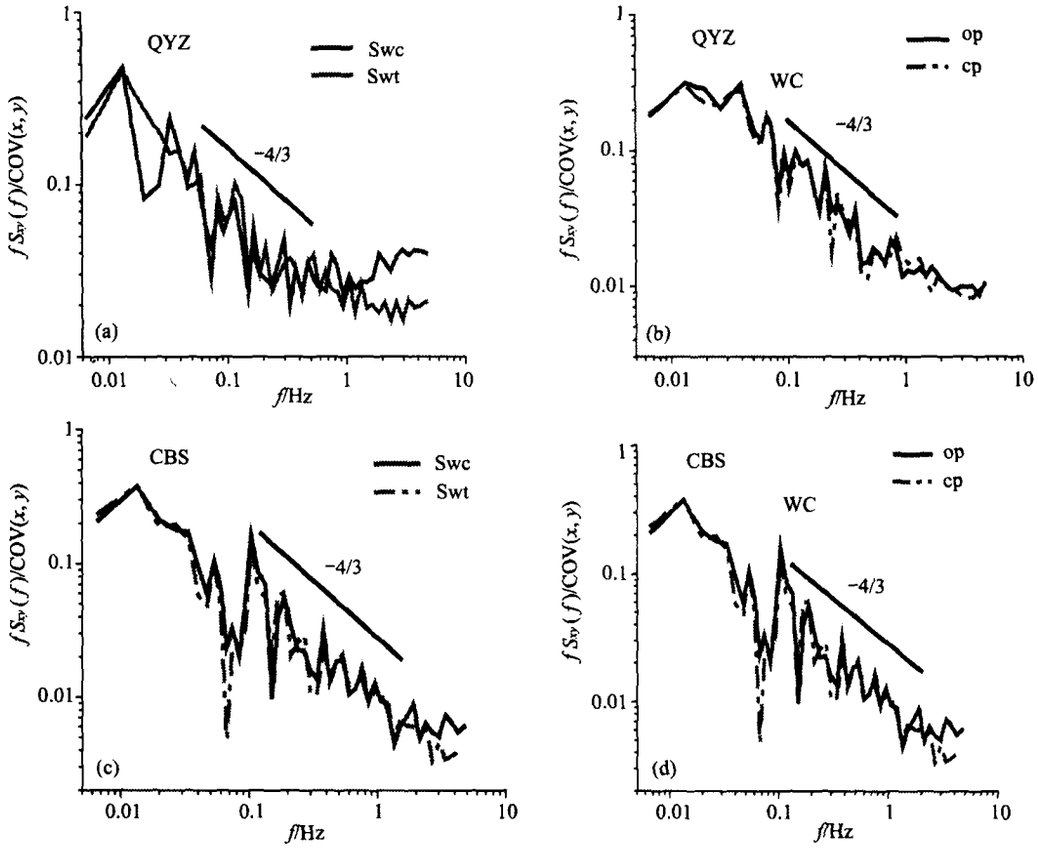

Fig. 5. (a) and (c) The comparison between WC cospectrum and WT cospectrum for OPEC, x and y denote vertical wind speed and CO_2 density, vertical wind speed and sonic anemometer temperature respectively. (b) and (d) the comparison between WC cospectrum of OPEC and that for CPEC, x and y denote the vertical wind speed and CO_2 density of OPEC and CPEC.

that of OPEC. The peak of cospectra was at 0.3 Hz for this period. Since the measurement was made above a forest, the frequency of the spectral peak would be lower than for above a crop field. This is an advantageous point of the close-path measurements over tall vegetation, because frequency bands contributing to the flux over tall vegetation shift to lower frequencies, which can mostly be covered by a slow response system. Leuning[8] found that the flux measurement by close-path analyzer at frequencies > 0.1 Hz was significantly less than for the open-path analyzer, because density fluctuations were damped by the sampling tube at these frequencies. In this study, when the frequencies > 1 Hz, the flux measurement by the close-path was less than that by the open-path.

3.3 Comparison of flux

The open-path flux measurement was used as the independent variable[9], and the close-path flux measurement results were evaluated. According to mean half-hour data of flux, fig. 6 compares the CO_2 and H_2O flux with two analyzers by linear regression. Fig. 6 shows that the slope of simulated line was larger than 0.8, and it was nearly 1 of water flux in QYZ. So the attenuation of the fluctuations along the sampling tube of the close-path analyzer did not result in significant underestimation. The open-path flux measurement was used as a standard of comparison, and CO_2 and H_2O flux of CPEC were 84% and 100% in QYZ, 80% and 86% in CBS, respectively. The correlation between the two systems measurement over

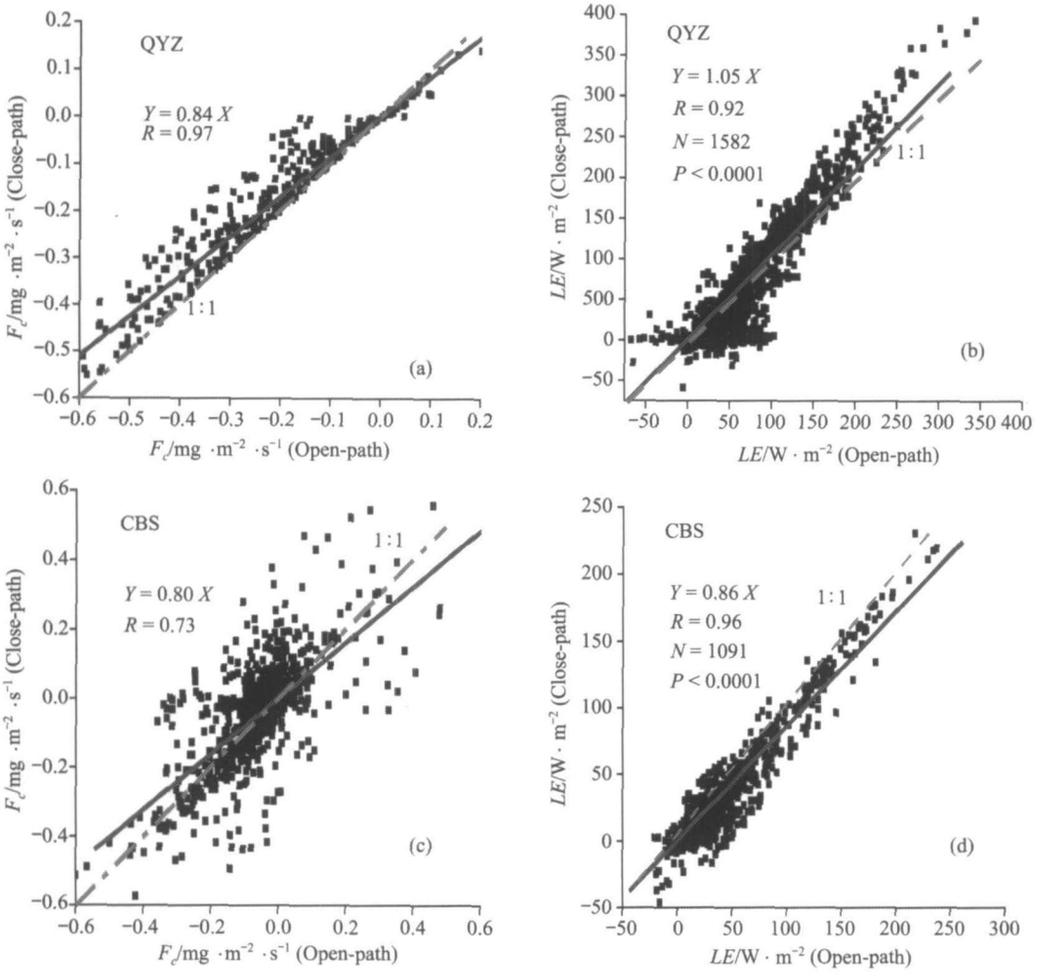

Fig. 6. Comparative CO_2 and H_2O flux measurements of the close-path and the open-path analyzers. (a) The comparison of CO_2 flux in QYZ station; (b) that of latent flux in QYZ station; (c) that of CO_2 flux in CBS station; (d) that of latent flux in QYZ station.

H_2O flux was better than that for CO_2. The underestimation resulted from the attenuation of both CO_2 and H_2O flux in QYZ was all smaller than that in CBS, and it may be caused by system error or different environmental controls.

The diurnal variations in CO_2 fluxes measured by the open-path analyzer were compared with those measured by the open-path analyzer in fig. 7(a)—(d). In the two sites, the CO_2 and latent heat flux from the close-path analyzer were in good agreement with those from the open-path analyzer, and the agreement was apparent in both the nighttime and the daytime, therefore, it suggested that the measurement of two different systems was reliable. In September and October, the diurnal variation was very obvious in QYZ, however, it was only in September that the diurnal variation was clear, but in October it was not.

4 Conclusions

Through computing the lag time of close-path analyzer, analyzing the spectra and cospectra of time-series data, and making the comparison of flux, some conclusions were drawn as the following:

(i) The delay time for CO_2 and H_2O determined by the maximum covariance between the vertical wind and CO_2 (H_2O) concentration was about 7.0 s—8.0 s

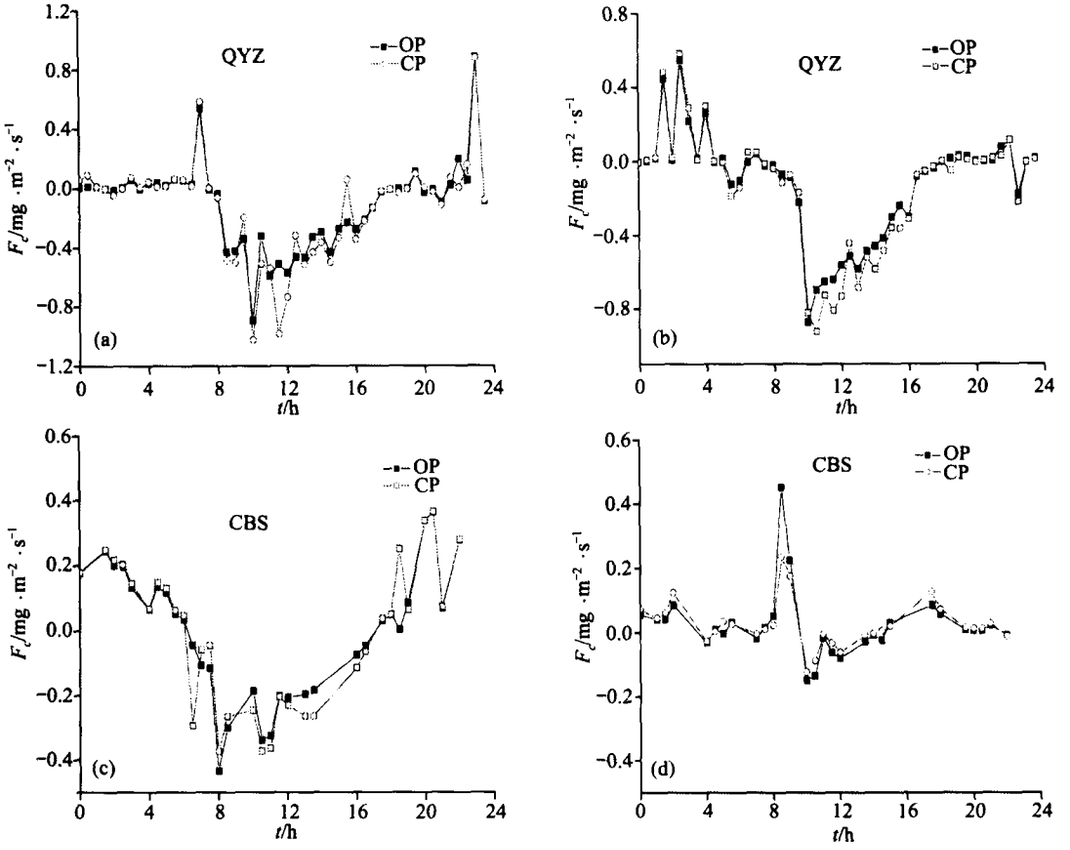

Fig. 7. CO_2 flux diurnal variations of the close-path and the open-path analyzers. (a) On September 30, 2003 in QYZ station; (b) on October 21, 2003 in QYZ station; (c) on September 22, 2003 in CBS station; (d) on October 20, 2003 in CBS station.

for CO_2, and about 8.0 s—9.0 s for H_2O at QYZ and CBS. For the increased interaction of water vapor with the internal surfaces of the tubing, the delay time for H_2O was larger than that of CO_2

(ii) The spectrum of ρ_{CO_2}, w, u, v from the open-path, close-path and 3D sonic anemometer was consistent with the expected −2/3 slope, and the co-spectra all showed the expected slope of −4/3 in the internal subrange. The cospectrum of vertical wind speed and CO_2 density was very similar. The cospestrum of vertical wind speed and CO_2 density was consistent measured by the open-path analyzer with the cospectrum of vertical wind speed and sonic anemometer temperature, and it showed that there was no significant loss in the measured CO_2 flux due to separation between the open-path analyzer and the sonic anemometer.

(iii) The open-path flux measurement was used as a standard of comparison, the CO_2 flux measured with the close-path sensor was about 84% at QYZ, about 80% at CBS, and the latent heat flux was balanced of two systems at QYZ, 86% at CBS. From the flux measurement difference between the open-path and close-path analyzers, we know that the attenuation of turbulent fluctuations in flow through tube of CPEC affected H_2O flux more seriously than CO_2 flux. The difference of two measurement systems were larger at site CBS than in QYZ. The diurnal variations of CO_2 and latent heat flux from the close-path analyzer were in good agreement with those from the open-path analyzer.

(iv) From all analyses, we could conclude that in two sites the measurement results of OPEC and CPEC were reliable. Therefore, in practice the two different

systems should be integrated to compensate the missing data.

Acknowledgements This work was supported by the Chinese Academy of Sciences and the Ministry of Science and Technology (Grant Nos. 2002CB412500 and KZCX1-SW01). We also appreciate the technical assistance provided by Campbell Scientific Inc., U.S.A., and its representative, the Tempo company in China.

References

1. Desjardins, R. L., A technique to measure CO_2 exchange under field conditions, Int. J. Biometeorol., 1974, 18: 76—83.
2. Desjardins, R. L., Lemon, E. R., Limitations of an eddy covariance technique for the determination of the carbon dioxide and sensible heat fluxes, Bound. Lay. Meteorol., 1974, 5: 475—88.
3. Jones, E. P., Zwick, H., Ward, T. V., A fast response atmospheric CO_2 sensor for eddy correlation flux measurement, Atmos. Environ., 1978, 12: 845—851.
4. Bingham, G. E., Gillespie, C. H., McQuaid J H. Development of a miniature, rapid response CO_2 sensor, Lawrence Livermor, National Lab, Report UCRL-52440, 1978.
5. Brach, E J., Desjardins, R. L., StAmour, G. T., Open path CO_2 analyser, J. Phys. E. Sci. Instrum., 1978, 14: 1415—1419.
6. Ohtaki, E., Matsui, T., Infrared device for simultaneous measurements of fluctuations of atmospheric CO_2 and water vapor, Boun. Lay. Meteorol., 1982, 24: 109—119.
7. Leuning, R., Moncrieff, J., Eddy-covariance CO_2 Flux measurements using open- and closed-path CO_2 analyzers: corrections for analyzer water vapor sensitivity and damping of fluctuations in air sampling tubes, Boundary-Layer Meteorol., 1990, 53: 63—76.
8. Leuning, R., King, K. M., Comparison of eddy covariance measurements of CO_2 fluxes by open- and closed-path analyzers, Boundary-Layer Meteorol., 1992, 59: 297—311.
9. Suyker, A. E., Verma, S. B., Eddy correlation measurement of CO_2 flux using a closed-path sensor: Theory and field tests against an open-path sensor, Boundary-Layer Meteorol., 1993, 64: 391—407.
10. Lee, X., Black, T. A., Novak, M. D., Comparison of flux measurements with open- and closed-path gas analyzers above an agricultural field and a forest floor, Boundary-Layer Meteorol., 1994, 67: 195—202.
11. Leuning, R., Judd, M. D., The relative merits of open- and closed-path analyzers foe measurements of eddy fluxes, Global Changes Biology., 1996, 2: 241—253.
12. Yasuda, Y., Watanabe, T., Comparative measurements of CO_2 flux over a forest using closed-path and open-path CO_2 analysers, Boundary-Layer Meteorol., 2001, 100: 191—208.
13. Baldocchi, D. D., Hicks, B. B., Meyers, T. P., Measuring biosphere-atmosphere exchanges of biologically related gases with micrometeorological methods, Ecology, 1988, 69: 1331—1340.
14. Paw, U. K., Baldocchi, D. D., Meyers, T. P. et al. Correction of eddy covariance measurements incorporating both advective effects and density fluxes, Boun-Lay. Meteorol., 2000, 97: 487—511.
15. Reynolds, O., On the dynamical theory of incompressible viscous fluies and the determination of criterion, Phil. Trans. Roy. Soc. London, 1895, A174: 935—82.
16. Webb, E. K., Pearman, G. I., Leuning, R., Correction of flux measurements for density effects due to heat and water vapour transfer, Quart. J. Roy. Meteorol. Soc., 1980, 106: 85—100.
17. Massman, W. J., Lee, X., Eddy covariance flux corrections and uncertainties in long term studies of carbon and energy exchanges, Agric. For. Meteorol., 2002, 113: 121—144.
18. Garratt, J. R., Limitations of the eddy correlation technique for determination of turbulent fluxes near the surface, Bound.-Lay. Meteorol., 1975, 8: 255—259.
19. Goulden, M. L., Crill, P. M., Automated measurements of CO_2 exchange at themoss surface of a black spruce forest, Tree Physiol., 1997, 17: 537—542.
20. Lee, X., Black, T. A., Hartog, G. et al., Carbon dioxide exchange and nocturnal processes over a mixed deciduous forest, Boundary-Layer Meteorol., 1996, 81: 13—29.
21. Song, X., Liu, Y., Xu, X. et al., The comparesion study on change dioxide, water and heat fluxes in winter and spring over the forest ecosystem in red earth hilly zone, Recourses Sciences (in Chinese), 2004, 26(3): 96—104.
22. Li, J., Pei, T., Li, X. et al., Model of soil saturated infiltration coefficient and effective porosity in forest catchment, Chinese Journal of Applied Ecology (in Chinese), 1998, 9(6): 597—602.
23. Jin, M., Guan, D., Zhu, T., Spectral characteristics of solar radiation in broadleaved Korean pine forest in Changbai Mountains, Chinese Journal of Applied Ecology (in Chinese), 2000, 11(1): 19—21.
24. Wu, G., Liang, X., Zhang, X., Height niche of some tree species in the Korean pine-broad-leaved forest on Changbai Mountains, Chinese Journal of Applied Ecology (in Chinese),1999, 9(3): 262—264.
25. Ding, Y., Jiang, C., The Signal Process of Meteorology Data Time Serials (in Chinese), Beijing: Meteorology Press, 1998.
26. Kaimal, J. C., Finnigan, J. J., Atmospheric Boundary Layer Flows: Their Structure and Measurement, Oxford University Press, 1994, 289.
27. Wyngaard, J. C., Cote, O. R., Cospectral similarity in the atmospheric surface layer, Quarterly Journal of the Royal Meteorological Society, 1972, 98: 590—603.